Platinum Nanoparticles at Mica Surfaces

Zhiqun Lin and Steve Granick*

Departments of Materials Science and Engineering, Chemistry, and Physics, University of Illinois, Urbana, Illinois 61801

Received April 28, 2003. In Final Form: June 6, 2003

We report a systematic study of factors that influence the incidence of platinum (Pt) nanoparticles produced by the standard method of cutting mica sheets into shapes using a hot platinum wire. Related findings in prior literature are confirmed. Characterization by AFM (atomic force microscopy) shows that fewer particles were produced the thinner the Pt wire and that the density and size of particles were substantially less when using Pt wire not previously used to cut mica. In optimal cases, using 0.0125 in. diameter wire, we obtained ∼0.1% surface coverage; the mean particle height of particles was ∼2.3 nm, and the mean diameter, 15 nm. After detachment from a backing sheet, the particle abundance was reduced by a factor of roughly 2. For Pt wires of the same diameter, the abundance of particles as a function of mica thickness and location relative to the wire was studied. The identification of these particles as Pt was confirmed using a combination of TEM (transmission electron microscopy) and Rutherford backscattering (RBS). After applying normal loads relevant to conditions in the surface forces apparatus, up to 5 MPa, we conclude from AFM characterization that the particles were not deformed by normal load and that their indentation into the underlying mica substrates was negligible. Cutting mica with hot iridium (Ir) rather than Pt wire also produced nanoparticles. Finally, FECO interference fringes (fringes of equal chromatic order) between cleaved mica sheets in close contact were contrasted with and without nanoparticles present. Implications for surface forces measurements are discussed tentatively.

Introduction

The surface force apparatus (SFA) has been used for more than a quarter century to measure forces between two crossed cylindrical surfaces in liquid media as a function of their separation.[1−7] Shear devices have been further developed in conjunction with the SFA technique.[8−11] The basis of these methods is that surface roughness should be negligible relative to the surface separation. To this end, single crystals of muscovite mica are prepared by cleavage to be free of steps; therefore, it has been supposed they were atomically smooth. Recently it was discovered that this was not necessarily so. Mica as commonly prepared by cutting with a hot platinum wire is reported to possess ≈0.05−1% surface coverage of nanometer-sized platinum particles.[12−15] This is probably because the vapor pressure of platinum is not negligible at the melting temperature of mica, 1320 °C (≈10^{-7} Torr, i.e., ≈0.1 monolayers per second). While the incidence of nanoparticles and their size surely differ from laboratory to laboratory and probably from experiment to experiment, and they are reported to be dislodged in acidic water, it is not easy to dismiss their conceivable presence in experiments that employed a hot platinum wire to cut mica substrates.

Use of a hot platinum wire in preparing mica sheets is so routine that it is seldom mentioned, in the literature, in descriptions of the experimental protocol. The main point is the need to detach atomically smooth regions of cleaved mica from surrounding mica on the larger sheet that has been cleaved. When a platinum wire is heated electrically to be red-hot or white-hot,[3] it melts where it touches and also conveniently burnishes the edges so that there is something to grip when handling the sheets later with tweezers. Because mica cut this way has uniform thickness, standard interferometric equations can subsequently be used to calculate surface separation after silvering the surfaces to form a Fabry−Perot interferometer,[1] and the complication of having surfaces of asymmetric thickness[16] is avoided. Use of platinum wire was standard until Frantz and Salmeron first discovered that this procedure appeared to lower the adhesion of mica sheets in air.[17] Christenson and co-workers reported the ensuing presence of nanosized particles.[12] Kohonnen, Christenson, and co-workers subsequently identified these particles to be platinum.[13] Independently, Heuberger and co-workers explored their consequences on surface forces and refractive index of molecularly thin fluids.[14] Mugele and co-workers explored their consequences for drainage of molecularly thin fluids.[15] This laboratory has found that the mechanical properties of confined nonpolar fluids

* To whom correspondence should be addressed.

(1) Israelachvili, J. N. *J. Colloid Interface Sci.* **1973**, *44*, 259.
(2) Israelachvili, J. N.; Adams, G. E. *Nature* **1976**, *262*, 774.
(3) Israelachvili, J. N.; Adams, G. E. *J. Chem. Soc., Faraday Trans.* **1978**, *74*, 975.
(4) Tabor, D.; Winterton, R. H. S. *Proc R. Soc. London A* **1969**, *312*, 435.
(5) Israelachvili, J. N.; Tabor, D. *Proc R. Soc. London A* **1972**, *331*, 19.
(6) Israelachvili, J. N. *Intermolecular and Surface Forces*; Academic Press: London, 1991.
(7) Israelachvili, J. N. In *Handbook of Micro/Nanotribology*; Bhushan, B., Ed.; CRC Press: Boca Raton, FL, 1995.
(8) Peachey, J.; Alsten, J. v.; Granick, S. *Rev. Sci. Instrum.* **1991**, *62*, 463.
(9) Alsten, J. v.; Granick, S. *Phys. Rev. Lett.* **1988**, *61*, 2570.
(10) Alsten, J. v.; Granick, S. *Langmuir* **1990**, *6*, 876.
(11) Homola, A. M.; Israelachvili, J. N.; McGuiggan, P. M.; Gee, M. L. *J. Tribol.* **1989**, *111*, 675.
(12) Ohnishi, S.; Hato, M.; Tamada, K.; Christenson, H. K. *Langmuir* **1999**, *15*, 3312.
(13) Kohonen, M. M.; Meldrum, F. C.; Christenson, H. K. *Langmuir* **2003**, *19*, 975.
(14) Heuberger, M.; Zach, M. *Langmuir* **2003**, *19*, 1943.
(15) Becker, T.; Herminghaus, S.; Mugele, F. Private communication.
(16) Horn, R. G.; Smith, D. T. *Appl. Opt.* **1991**, *30*, 59.
(17) Frantz, P.; Salmeron, M. *Tribol. Lett.* **1998**, *5*, 151.

10.1021/la034716u CCC: $25.00
Published on Web 07/16/2003

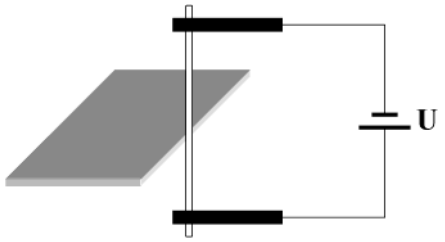

Figure 1. Schematic representation of the procedure to cut cleaved mica sheets to size using a hot platinum wire. The vertically oriented platinum wire is heated by a constant current power supply (U), and the horizontally configured mica sheets are brought into contact with it. This procedure is performed within a laminar flow cabinet, and care is taken not to disturb laminar air flow.

are significantly different when mica is prepared by cleaving with adhesive tape rather than cut to shape using platinum wire.[18]

This is not the only method to prepare atomically smooth surfaces of mica, however. Mica can be cleaved by placing adhesive tape on top and removing it rapidly, as described by Frantz and Salmeron.[17] Alternatively, cleaved sheets can be detached from the surrounding mica by cutting with surgical scissors as described by Zach and Heuberger.[14]

Here we consider the factors that control the abundance of platinum nanoparticles, leaving to other studies questions of how subsequent surface force measurements are affected. First, we study the abundance of Pt nanoparticles as a function of mica film thickness and location. Then we compare the surface qualities of mica films prepared with new and old hot Pt wires. The possibility of dislodging Pt nanoparticles is also investigated and found to be consistent with those reported in the literature. We discuss the possibility that, under the application of repulsive surface forces, Pt particles might indent into the mica substrates. Finally, we investigate their influence on FECO fringes (fringes of equal chromatic order).

Experimental Section

ASTM V-2 ruby-red muscovite (mica) ($KAl_2(Si_3AlO_{10})(OH)_2$), grade 3 or 4, was purchased from Lawrence and Co. (MA) and cleaved by hand in a laminar-flow hood. Thin mica films suitable for experiments in a surface force apparatus (SFA) have a pale yellow or light green color (1−5 μm thick). To protect the cleaved mica from airborne contaminants resulting from body fluids and fragrances, polyethylene gloves (VWR Scientific) were routinely worn during all manipulation of the mica.

Following cleavage of mica sheets to the desired thickness, a hot platinum wire was employed to separate these regions from those that surrounded them. The wire, about 6 cm long, was mounted vertically between two electrodes of a constant current power supply and heated by current to the point that it sliced smoothly through micrometer-thick mica sheets as they were brought manually into contact with it (reminiscent of a hot knife passing through butter) while oriented horizontal to the laboratory frame of reference. Detached sheets with area of a few square centimeters were gripped at the edges by clean tweezers and laid onto a thicker "backing" sheet of freshly cleaved mica, whose large thickness and larger area made it easy to handle. Figure 1 shows a sketch of the experimental logistics.

All these operations were performed within a laminar flow cabinet with HEPA filters of size 0.3 μm (NuAire). Care was taken to maintain efficient air flow within the laminar flow cabinet.

(18) Zhu, Y. X.; Granick, S. Submitted.

Deposition of silver for interferometry was performed (using an AJA sputtering unit) following these ministrations. The Pt and iridium (Ir) wires were purchased from the Alfa Aesar Corp. The diameters of the wires used were 0.02 and 0.0125 in. for Pt and 0.02 in. for Ir.

To investigate the possibility of dislodging nanoparticles by immersion in liquid, first the mica films were immersed either in acid water (pH = 3, HCl) for 5 min or in deionized water for 0.5 h followed by another 14.5 h with agitation. To investigate the possibility of dislodging particles with organic solvents, the mica films were treated in the same way with cyclohexane and octamethylcyclotetrasiloxane (OMCTS) for 5 min and 1 h, respectively, with agitation. All films were then blown dry with dry N_2 gas in a laminar flow hood.

In attempts to determine the crystalline structure of the particles, they were also imaged in a transmission electron microscope. In earlier experiments (not shown), we were not successful in imaging Pt particles on mica, because diffraction from the mica overwhelmed the smaller signal from Pt. A more successful approach was to employ windows of silicon nitride (Si_3N_4). Silicon nitride is amorphous and transparent to electron beams. Thin sheets of Si_3N_4 (20 nm thick) were positioned 5 mm above a glowing Pt (or Ir) wire for 30 s. The samples were then used for transmission electron microscopy (TEM) studies using a Philips CM12 instrument in bright field, operated at 120 keV.

Chemical identification of the particles as platinum was confirmed using Rutherford backscattering (RBS). For these experiments, a piece of fresh mica backing sheet was exposed to glowing Pt wire for 30 min. A dark stain was observed at the mica surface, indicating that particles had been deposited. The RBS technique was then used to measure the composition profile at the mica surface. Rutherford backscattering was carried out at 2 MeV, 100 nA using $^4He^+$ ions at the angle $\beta = 22.5°$ (incident beam to surface normal) and detected at $\alpha + \beta = 52.5°$. The beam size was ~2 mm.

In experiments designed to test whether Pt nanoparticles deform under the influence of external load, two mica films were pressed against one another under pressures of 1, 3, and 5 MPa to mimic the loads typical of experiments in a surface forces apparatus. To ensure even distribution of the load across the contact zone, special care was taken to use smooth surfaces. To this end, lead weights were placed on top of an aluminum cylinder, this cylinder was placed against a single crystal of silicon wafer, and this in turn was pressed against two mica sheets that were laid on top of one another for a prescribed time. Following this protocol, the mica sheets were separated and the density and shape of particles on them were compared by AFM characterization.

The thickness of the mica sheets was measured using a Sloan Dektek 3 profilometer. The typical mica film thicknesses used in the studies were in the range 1−5 μm (thickness is specified below when describing particular experiments).

AFM studies were performed with a Digital Instrument D3100 scanning force microscope in the tapping mode using etched Si tips on cantilevers (Nanoprobe) with a spring constant stated by the manufacturer to be 45.88 $N \cdot m^{-1}$. The scan rate was ≈1 Hz, and the tapping frequency was 335 kHz. Although we acquired both phase images and height images, to conserve space, only the height images are shown below.

Results and Discussion

The following discussion aims first to characterize the factors on which the abundance of Pt nanoparticles depend and second to show how this problematical matter can be avoided. The principal characterization method (in addition to RBS and TEM) was AFM (atomic force microscopy) in the tapping mode. Seminal earlier measurements on this same question employed the contact mode instead.[12] We employ here the tapping mode, as it is less perturbative. The AFM images presented below necessarily pertain to limited areas but are illustrative of numerous other images that we also obtained.

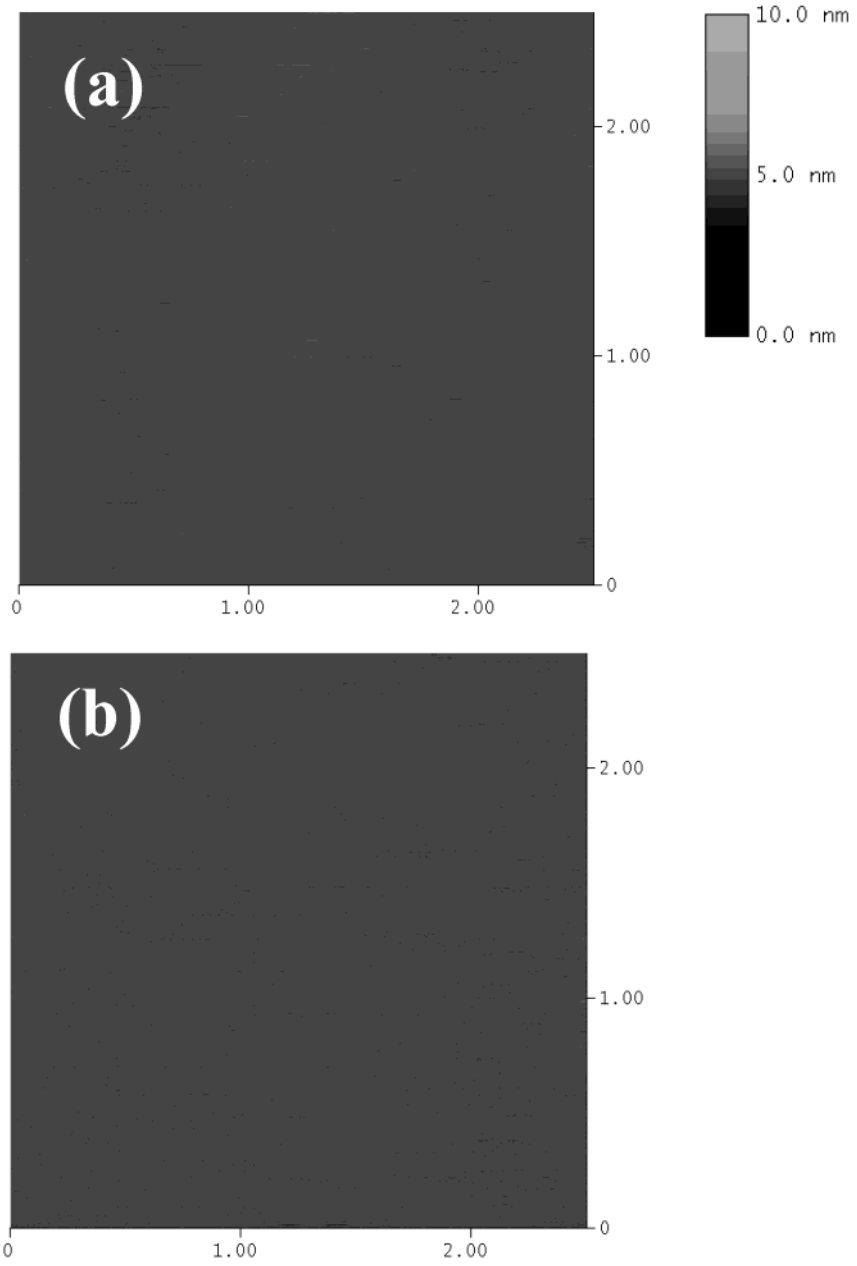

Figure 2. AFM scans (height images) of mica sheets obtained after (a) cutting them to size using surgical scissors or (b) cleaving them by detaching adhesive tape (Scotch tape). In both cases, the featureless background with a background of only thermal noise shows the absence of nanoparticles. Image sizes are 2.5μm × 2.5μm.

Surfaces Free of Nanoparticles. Several ways have been reported to obtain atomically smooth cleaved mica surfaces free of Pt nanoparticles.[14,17] Figure 2 shows mica surfaces prepared via two of these unconventional methods: (a) cut with surgical scissors after cleavage by otherwise the same procedures as when using a platinum wire, and (b) cleaved by detaching an adhesive tape previously placed on a mica sheet. The AFM images in Figure 2 show that both mica surfaces are featureless, consistent with findings in the literature.[14,17] These control experiments employed procedures essentially the same as those when we employed a hot platinum wire to cut the mica to shape. On this basis, we conclude that particles did not result from some adventitious other aspect of our preparation protocol but resulted from using the hot platinum wire.

Presence of Pt Nanoparticles. A typical AFM image of a mica surface cut using a hot platinum wire is shown in Figure 3. The cutting time was ∼15 s. This was the typical time for the experiments presented below, unless noted otherwise.

This mica was cut using a fresh (not previously used) Pt wire of 0.0125 in. diameter, and the image is of the top side, the side that during the cutting process was oriented upward while the horizontally oriented mica sheets were cut. The mica thickness was 2.74 μm. The presence of nanoparticles with ∼0.2% surface coverage is clearly evident in this height image. This is reduced to ∼0.1% surface coverage if the cleaved mica is placed on a backing sheet and then detached (see below). The mean height of particles is ∼2.3 nm with a mean diameter of 15 nm. These observations are broadly consistent with those of previous studies.[12,13] When using a platinum wire to cut mica, there is a tradeoff between using thin wire, which cuts quickly and most cleanly (but the heat of the electric current causes it to snap often, which is expensive because Pt is costly

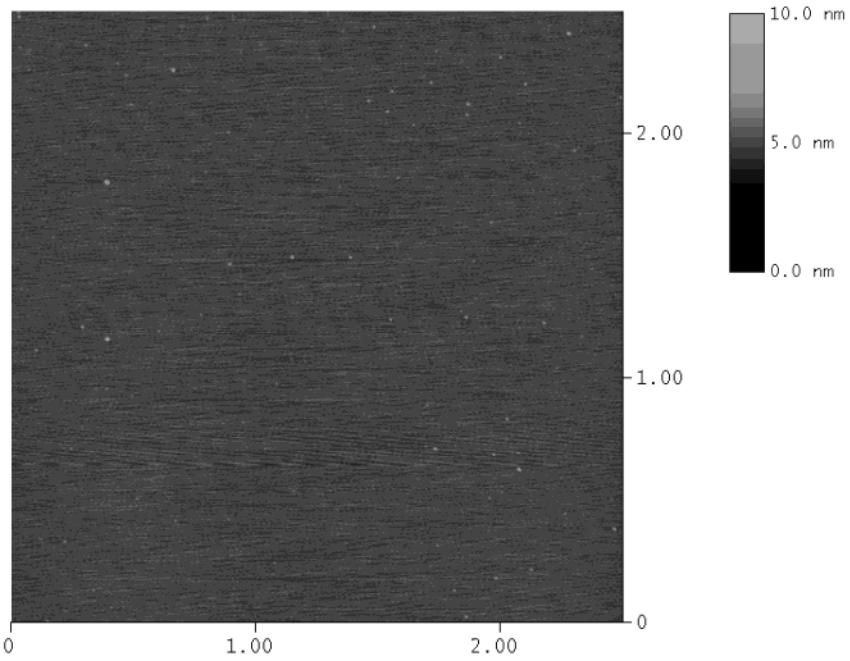

Figure 3. Mica of thickness 2.74 μm cut using a fresh Pt wire of 0.0125 in. diameter. During cutting, the mica was exposed to glowing Pt wire for ~15 s. The AFM image is of the top side, the side that during the cutting process was oriented upward while the horizontally oriented mica sheet was cut. The presence of nanoparticles with ~0.2% surface coverage is clearly evident in the height image. The mean diameter and height of the particles are 15 and 2.27 nm, respectively. The image size is 2.5 μm × 2.5 μm.

to replace), and using thicker wire (with converse advantages and disadvantages).

A systematic series of experiments using a fresh 0.02 in. diameter Pt wire showed that, in general, the particle density was ~4−5 times larger. This is understandable when one considers the larger surface area and consequent larger opportunity for sublimation than is the case when using 0.0125 in. diameter Pt wire. Figures 7−10 show examples of this; those figures are discussed below in connection with other items.

Note that a surface coverage of 0.1% is equivalent to a mean spacing between particles of 400 nm, which is less than the wavelength of light. Platinum nanoparticles spaced by less than the wavelength of light would therefore be undetected by the optical interference fringes used to image the contact area in a surface forces apparatus.

To confirm the presence of particles by an independent method, first TEM studies were performed. It should be pointed out that since mica films (1−5 μm) are much thicker than Pt particles, an electron beam hardly penetrates such a thick mica film in a TEM experiment. To circumvent this, we exposed Si_3N_4 windows, ~20 nm thick, to a glowing Pt wire for 30 s and then performed TEM imaging of the underside. Presumably in part because of the relatively large exposure time and in part because of different wetting characteristics on this different substrate, the surface coverage is larger than that for AFM images of particles on mica. Figure 4 unambiguously demonstrates the presence of particles. Our attempts to determine the crystalline microstructure by diffraction, especially whether the particles were single crystals or polycrystalline, were unsuccessful.

The chemical identification of particles as Pt was confirmed using Rutherford backscattering of helium ions (RBS) using a facility in the Center for Microanalysis of Materials at the University of Illinois. A strong signal from Pt at the known energy of 1.8 MeV is obvious in Figure 5.

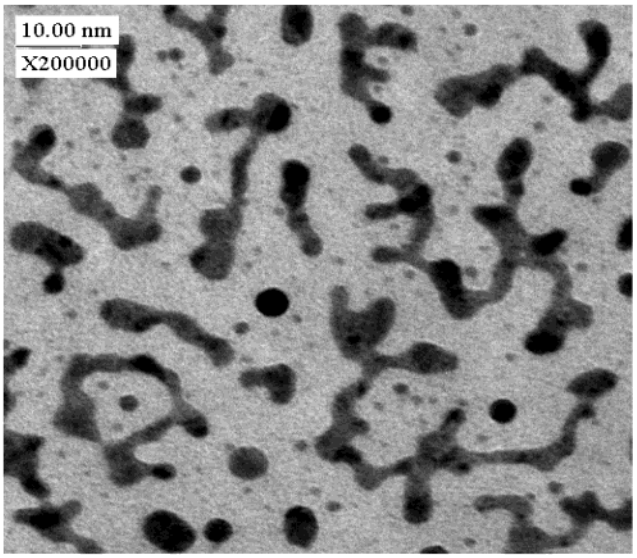

Figure 4. TEM (transmission electron microscopy) image demonstrating by an independent experiment than using AFM the presence of particles (dark spots) on Si_3N_4 windows (transparent to the electron beam) after exposure to glowing Pt wire for 30 s. Owing to different wetting on silicon nitride, the particle morphology differs from that on mica.

Issues that Influence the Abundance of Platinum Nanoparticles. Systematic experiments were then performed to determine the relative importance of various details of the experimental protocol. As already noted, care was always taken not to interfere with laminar air flow within the laminar flow cabinet.

Orientation of Mica Surface (up or down) during Cutting. For many years, a standard feature of the surface forces technique has been to employ the side of mica that faces upward after a horizontally oriented mica sheet is cut using a platinum wire. Figure 6 shows the AFM height image of the mica sheet oriented downward during cutting

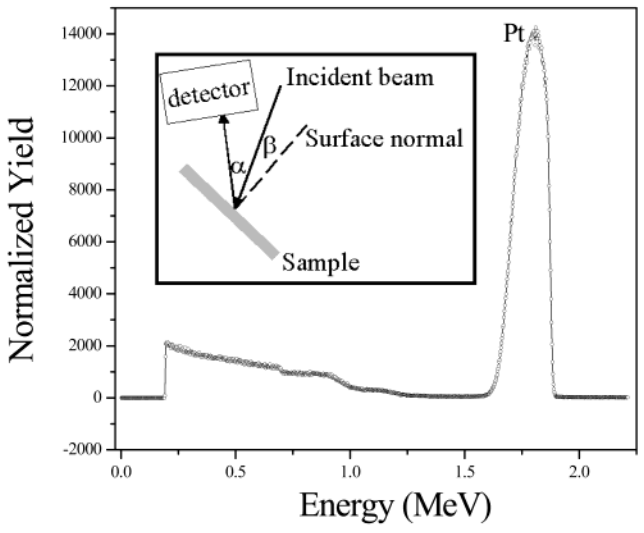

Figure 5. Rutherford backscattering (RBS) profile illustrating the presence of Pt particles after exposure of mica to glowing Pt wire for 30 min. The experimental geometry is shown in the inset.

with 0.0125 in. Pt wire. It is obvious that the particles are larger and more abundant than those in Figure 3 where the side was oriented upward during cutting (see caption of Figure 6 for quantification). Flakes of mica were sometimes observed (data not shown) when the mica was oriented downward during cutting but not when it was oriented upward.

Removal of Mica from Backing Sheet after Silvering. Typically a cleaved and cut mica sheet is placed clean-side down onto a thick mica "backing sheet" to protect the clean side and give it rigidity while it is coated with silver for subsequent optical interferometry.[1] Before an experiment, the cleaved and cut thin sheet is removed using tweezers and mounted into the surface forces apparatus. It is reasonable to inquire how detachment from the backing sheet alters the abundance of nanoparticles. We found the abundance to be about half after detachment and a tendency for the largest nanoparticles to be left behind on the backing sheet (data not shown).

Dependence on Mica Thickness. Typical surface forces experiments employ mica sheets that range from relatively thin to thick (the typical range is roughly 1−4 μm). To explore the dependence on this variable, a sheet of mica with a thickness variation of 1−4 μm was prepared by taking advantage of cleavage steps to produce the desired thickness gradient (see sketch in Figure 7).

Shown in Figure 8 are a series of AFM images showing the surface topography at positions where the film thickness was different. The presence of Pt nanoparticles as a function of mica thickness is summarized in Table 1. Contrary to the expectation of having more particles on thicker sheets due to the fact that thicker mica requires relatively more time to be cut, no significant differences were observed in terms of particle height, footprint, or surface coverage. This disagrees with a previously reported finding.[12] We believe the present finding is most likely because the mica sheets were cut using the same hot Pt wire through which passed the same electric current. As the electric current was the same in these experiments, so also was the cutting temperature.

Dependence on Location Relative to the Hot Platinum Wire. Typical surface forces experiments pertain to locations (Figure 9) on mica that are removed by 1−2 cm from the position where the mica was cut, so dependence on this variable was investigated next. The size of the mica film was 3.4 cm × 2.3 cm. Shown in Figure 10 is one set of representative AFM images out of many measurements made by scanning the sample from edge to center of the side oriented downward during cutting. A mica flake with a size of ∼200 nm can be seen in Figure 10d. Intuitively, we had expected to observe a progressive

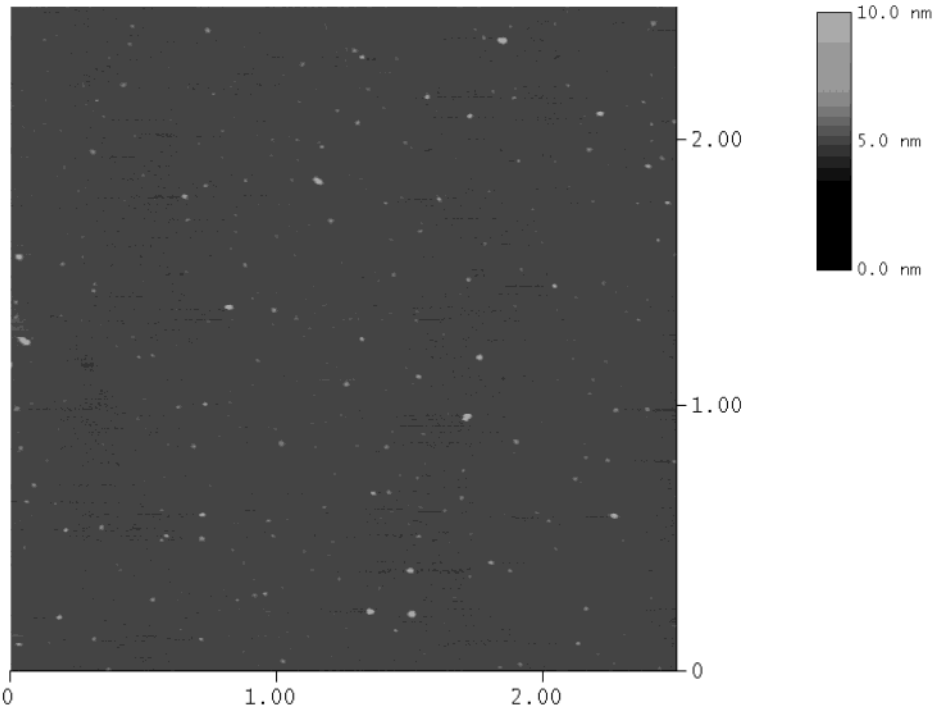

Figure 6. Comparison of upside and downside of Pt-cut mica. AFM height image of the mica sheet oriented downward during cutting (0.0125 in. fresh Pt wire). Compared to Figure 3, where the side was oriented upward during cutting, it is obvious that the particles are larger and more abundant. The particles were ∼5 times more abundant (∼1% surface coverage), and the mean diameter and height of the particles were 23 and 3.4 nm, respectively. Image size is 2.5 μm × 2.5 μm.

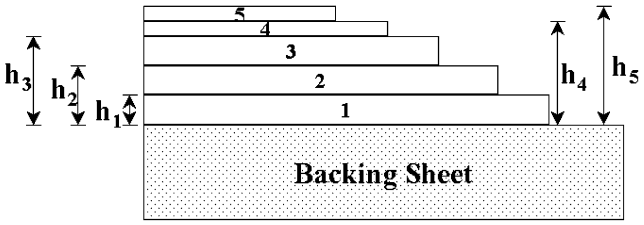

Figure 7. Sketch of the thickness gradient.

decrease of number density of particles from the edge (x, $y = 17, 7$) to the center ($x, y = 17, 11$) of the film. However, the images clearly show no systematic dependence on location across the surface. Table 2 summarizes the characteristic parameters of Pt nanoparticles in this study. These measurements were repeated after 3 days (data not shown), and no change of particle size or surface coverage was found, which indicates Pt nanoparticles at the mica surface were rather stable.

Dependence on Diameter and Age of the Platinum Wire. Next we compared findings using a fresh platinum wire and a wire that had been used many times. When a platinum wire is used repeatedly, it accretes molten mica. We found that a fresh Pt wire produces fewer, smaller particles. For a wire of thickness 0.02 in., the particle density using a fresh wire was ~1% (~2% using an aged wire; data not shown). The mean diameter was ~25 nm (~33 nm using an aged wire). The mean height was 2.5 nm (4.0 nm using an aged wire).

Furthermore, the particle density was less the thinner the platinum wire, which implies that the density should be even less if even thinner platinum wire (<0.0125 in.) were used.

Methods To Remove Pt Nanoparticles

It has been reported that Pt nanoparticles are dislodged by exposure to acid water.[19−21] This we confirmed after treating a melt-cut mica film with acid water (pH = 3, HCl) for 5 min (data not shown). Immersion in deionized water for an extended period (15 h) also dislodged particles from the surface. In contrast, no changes of particle size or abundance were observed after mica sheets were rinsed with deionized water, octamethylcyclotetrasiloxane (OMCTS), or cyclohexane.

Iridium rather than Platinum Wire

Reasoning that the melting point of mica (1320 °C) is close to that of platinum (1772 °C), next we investigated whether nanoparticles could be avoided using a noble metal whose melting point is higher. The melting point of iridium (Ir) is 2410 °C. By replacing Pt with Ir wire, we anticipated avoiding the production of nanoparticles, but both AFM studies on mica and TEM studies on Si_3N_4 exposed to the vicinity of a red-hot iridium wire demonstrated the presence of Ir nanoparticles (data not shown). Possibly this is because iridium oxides may have a higher vapor pressure than iridium metal, but no definitive explanation is offered at this time.

Deformation of Platinum Nanoparticles under Load

As the local pressure is high in a surface forces experiment since particles cover only a small fraction of the total surface, it is reasonable to inquire whether this pressure might press nanoparticles into the surface, thereby rendering the surface more smooth than would appear from the AFM images presented above. Here we estimate the indentation of Pt particles under normal loads typical of surface forces experiments.

Assume the nanoparticles are spherical in shape. From spherical nanoindentation theory the amount of indentation, h_e, can be given as the following[22]

$$h_e = \left(\frac{3F}{4E^* R^{1/2}}\right)^{2/3} \tag{1}$$

where F is the force exerted on a single particle and R is the particle radius. E^* can be written as[22−24]

$$\frac{1}{E^*} = \frac{1 - \gamma_{Pt}^2}{E_{Pt}} + \frac{1 - \gamma_{mica}^2}{E_{mica}} \tag{2}$$

where E_{Pt}, E_{mica} and γ_{Pt}, γ_{mica} are the elastic moduli and Poisson's ratios of Pt and mica, respectively. The surface coverage of Pt nanoparticles was ~1% from AFM studies. Thus, the number of Pt nanoparticles at the mica surface is

$$N_{Pt} = \frac{1\%A}{\pi R^2} \tag{3}$$

where A is the area to which load was applied. So the force exerted on a single Pt particle is

$$F = \frac{F'}{N_{Pt}} = \frac{PA}{N_{Pt}} \tag{4}$$

Substituting the relevant parameters of $E_{Pt} \sim 170$ GPa,[25] $E_{mica} \sim 34.5$ GPa,[26] $\gamma_{Pt} \sim 0.39$,[25] $\gamma_{mica} \sim 0.205$,[26] and $P \sim 5$ MPa into eqs 1−4, the indentation at this load is $h_e = 0.11R \ll 2R$. For the radius of a nanoparticle ~ 10 nm, h_e is ~1.1 nm. This signifies that indentation of Pt particles is small relative to the particle size.

A related question was whether high local pressures might deform the particles plastically, which would smoothen them. The yield stress is estimated to be 14 MPa for polycrystalline platinum[27] and 125−165 MPa for single-crystal platinum.[27] The latter is likely to be closer to the situation for these particles, whose small size should discourage the presence of dislocations. This was supported by our AFM measurements (data not shown) where controlled pressures were applied using the methods described in the Experimental Section. The shapes of the platinum particles were compared by AFM characterization before and after applying pressure. Macroscopic pressures of 1, 3, and 5 MPa were applied (these pressures refer to the load divided by the geometrical area of the mica). No changes were observed in the mean particle diameter or height.

(19) Kohonen, M. M.; Christenson, H. K. *Langmuir* **2000**, *16*, 7285.
(20) Christenson, H. K. *J. Phys. Chem.* **1993**, *97*, 12034.
(21) Christenson, H. K. *J. Colloid Interface Sci.* **1988**, *121*, 170.
(22) Fischer-Cripps, A. C. *Nanoindentation*; Spinger Verlag: New York, 2002.
(23) Savvides, N.; Bell, T. J. *J. Appl. Phys.* **1992**, *72*, 2791.
(24) Mencik, J.; Quandt, E.; Munz, D. *Thin Solid Films* **1996**, *287*, 208.
(25) Harting, M.; Ntsoane, T. P.; Bucher, R. *Adv. Eng. Mater.* **2002**, *4*, 607.
(26) Matsuoka, H.; Kato, T. In *International Tribology Conference*; Yokohama, 1995; p 93.
(27) *ASM Handbook Vol 2: Properties and Selection: Nonferrous Alloys and Special Purpose Materials*; ASM International: 1991.

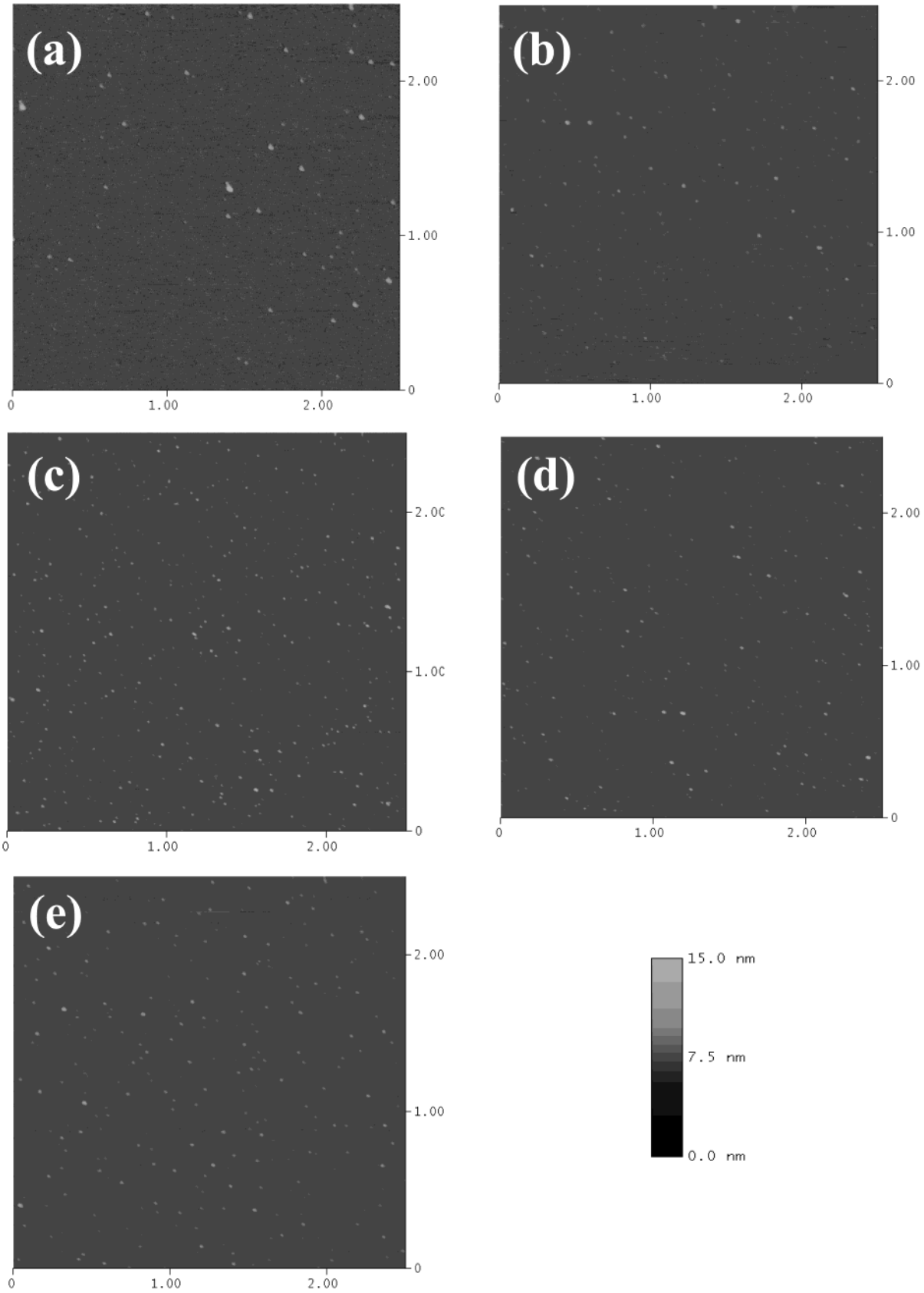

Figure 8. Dependence on mica thickness. A sheet of mica with thickness variation in the range 1−4 μm was prepared by taking advantage of cleavage steps to produce the thickness gradient shown in the sketch in Figure 7. Thickness was characterized by profilometry. The platinum wire diameter was 0.02 in. Panels a−e show AFM height images of surface topography at positions of different mica film thickness. The thicknesses of the mica layers were (a) ∼1.17, (b) ∼1.95, (c) ∼3.34, (d) ∼3.45, and (e) ∼3.53 μm, respectively. The results are summarized in Table 1. By performing this deposition onto a gradient of thickness in the same experiment, we controlled for conceivable variations between platinum wires and the electric current passing through them. The image sizes are 2.5 μm × 2.5 μm.

Table 1. Pt Nanoparticle Abundance on Mica with a Thickness Gradient[a]

layer no.	film thickness (μm)	peak height, h_{max} (nm)	lateral size (nm)	surface coverage (%)	rms roughness (nm)
1	1.17	8.77	26.35	~0.5−1	0.42
2	1.95	6.22	19.64	~1	0.30
3	3.34	7.94	15.84	~1−1.5	0.26
4	3.45	7.54	17.57	~1	0.20
5	3.53	5.25	15.84	~1	0.19

[a] For experimental parameters, see caption of Figure 8.

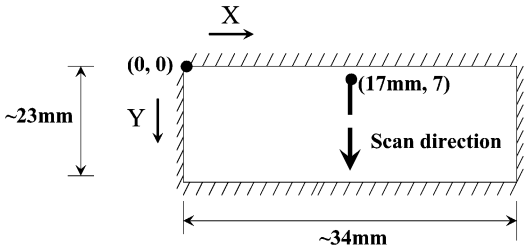

Figure 9. Sketch of the AFM sample stage that was moved in a program-controlled manner to produce exact changes of location while studying a mica sheet with dimensions 3.4 cm × 2.3 cm.

Table 2. Pt Nanoparticle Abundance as a Function of Location Relative to the Glowing Platinum Wire[a]

location (x, y) (mm, mm)	peak height,[b] h_{max} (nm)	lateral size (nm)	surface coverage (%)	rms roughness[b] (nm)
(17, 7)	7.23	24.46	~1	0.23
(17, 9)	9.53	24.46	~1	0.34
(17, 11)	8.04	24.46	~1	0.31
(17, 13)	25.15	30	~1	0.70
(17, 16)	6.21	28.35	~1	0.41

[a] For experimental parameters, see caption of Figure 10. [b] Note: The peak height, h_{max}, and rms roughness for the location x, y = 17, 13 were larger than others due to the presence of a mica flake, as mentioned in the text.

Comparison of Optical Interference Fringes with and without Nanoparticles Present

Platinum nanoparticles spaced laterally by less than the wavelength of light are not visible directly using the optical interference fringes used to image the contact area in the surface forces apparatus. But it is reasonable that their presence should modulate FECO fringes nonetheless. To explore this issue, white light was shone through the Fabry−Perot interferometer constructed by silvering the back-sides of the mica sheets, and the FECO fringes were analyzed.

We controlled for unwanted variations by performing experiments using the *same* sheets of cleaved mica, cut using surgical scissors to be particle-free. Interference fringes were compared: in one case, for a portion of mica that was never exposed to platinum wire and, in a second case, for a portion of mica that was exposed to glowing platinum wire to produce a surface density of ~2% nanoparticles. In both cases the mica sheet was subsequently cut in two, the dry halves were placed together as a sandwich, and the FECO fringes were imaged using a CCD (charge coupled detector).

Figure 11 compares the interference fringes for a typical case. The main figure shows a single fringe, and the inset shows an expanded view of four fringes. Note that birefringence of mica causes each fringe to split into two components, β and γ. In this raw data, one observes a shift of interference fringes toward longer wavelength for mica exposed to Pt wire, and also diminished interference intensity and fringe broadening. The optical height of Pt particles can be calculated on the basis of eq 5

$$d = \frac{\lambda^\circ_{n-1}}{2n_{mica}(\lambda^\circ_{n-1} - \lambda^\circ_n)}(\lambda_n - \lambda^\circ_n) \qquad (5)$$

where λ°_n, λ°_{n-1}, λ_n, and n_{mica} are the wavelengths of the nth and $(n - 1)$th fringes of pure mica/mica in-contact, the wavelength of the nth fringe of mica in-contact, and the refractive index of mica, respectively. Substituting the relevant experimental parameters of λ°_n = 534.63 nm, λ°_{n-1} = 543.05 nm, λ_n = 534.80 nm, and n_{mica} = 1.582 into eq 5, the height obtained is 3.47 nm, which is broadly consistent with the values in AFM studies. In performing this calculation, the fringes were fit to the Gaussian peaks shown in Figure 12. The comparison makes clear that the fringes were significantly broadened by the presence of Pt nanoparticles, with the full width at half-maximum (fwhm) taking the values specified in the figure caption.

These data may point the way to understanding how to reconcile the presence of Pt nanoparticles with the fact that experiments using the surface forces apparatus show significant variations of force when the surface spacing is varied by 0.1−0.2 nm—in other words, forces change when mica spacing is altered by quantities that are significantly less than the height of nanoparticles. The measured interferometric thickness appears to be some kind of average of the ~99% of the surface that is free of particles and the ~1% that is not.

Prospects

In agreement with findings from several other groups,[12−15] we have found that cutting mica with a hot platinum wire produces nanoparticles. Their abundance varies by more than an order of magnitude depending on experimental details that here we describe systematically.

It would be fair for a reader to inquire to what extent platinum nanoparticles have contributed to the many surface forces measurements that one finds in the literature. It is to be expected that surface roughness would impede the layering of fluids, which is the assembly of confined molecules into discrete layers parallel to solid surfaces. Yet surface forces measurements have reported layering for a long time. Preliminary experiments from this laboratory using mica that was demonstrably free of nanoparticles show distinctions in surface forces that can be understood as having reduced surface roughness; enhanced layering is observed when molecularly thin films of a simple globular-shaped molecular fluid (OMCTS) are confined between atomically smooth sheets of mica cleaved by tape-cleaving.[18] An intriguing aspect is the correlation of higher friction with less equilibration of the confined fluid in these experiments,[18] which calls attention to the salient influence on friction of surface heterogeneity.

The surface forces community is at an early stage of assessing the consequences of a dilute concentration of nanoparticles on mica surfaces, and there is much work left to be done.

One could argue that surface forces are trivial consequences of particles bumping into opposing surfaces, but it is useful to keep in mind that this would be inconsistent

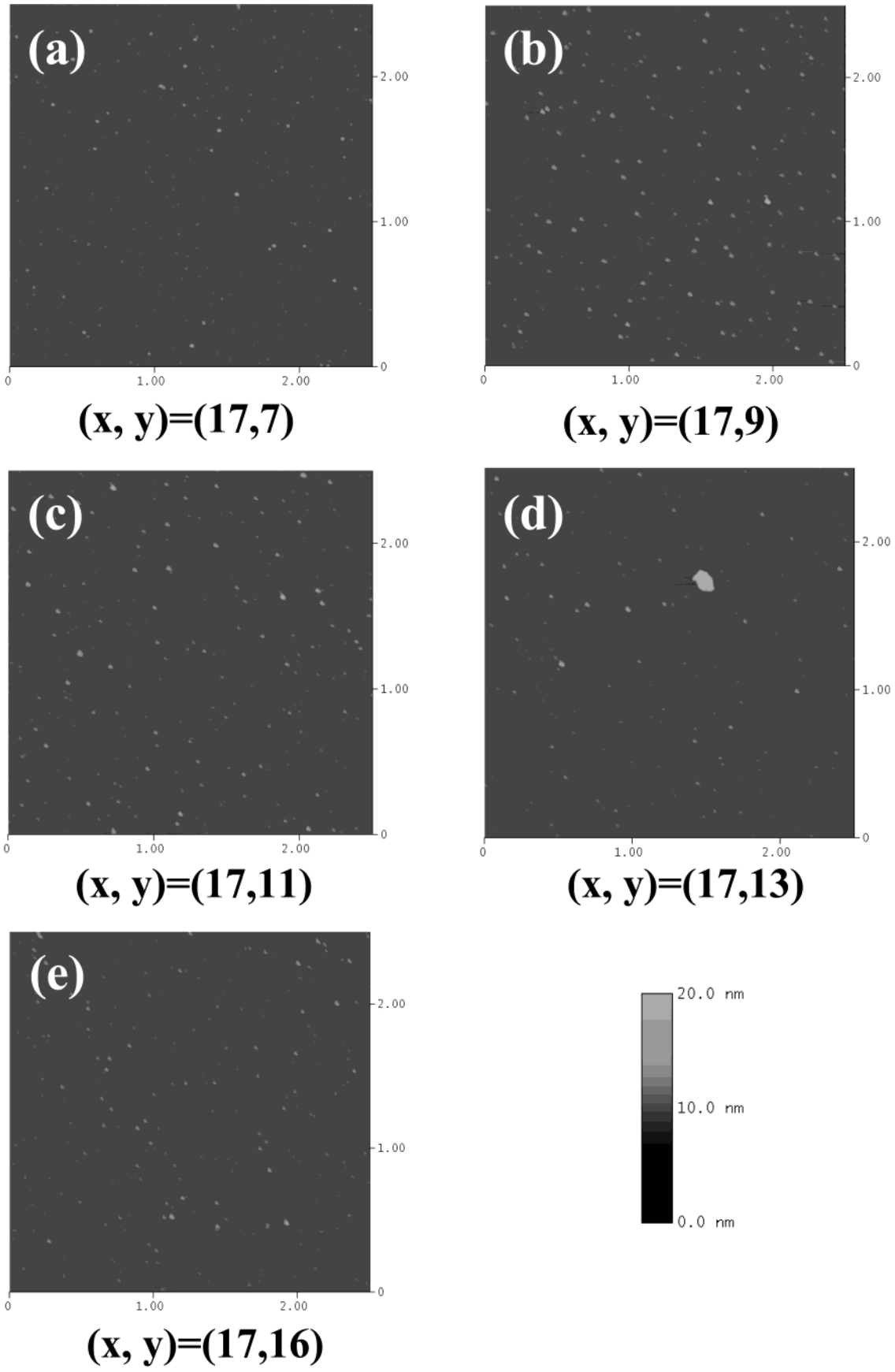

Figure 10. Dependence on location (as shown in Figure 9) relative to the glowing platinum wire during cutting, showing the side oriented downward during cutting. The mica sheets (~1.11 μm thick) were cut using Pt wire of 0.02 in. diameter. This is a set of representative AFM images out of many measurements made by scanning the sample from edge to center. A mica flake with a size of ~200 nm can be seen in part d. The images show no systematic dependence on location across the surface. Table 2 quantifies these findings. Image sizes are 2.5 μm × 2.5 μm.

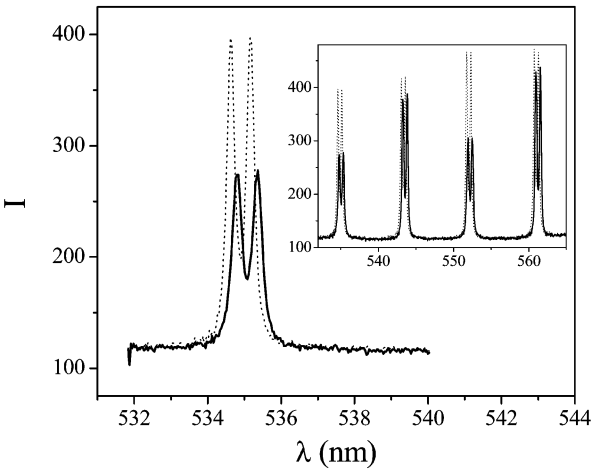

Figure 11. Interference fringes of mica/mica in dry contact without (dotted lines) and after (bold lines) exposure to Pt wire. Intensity is plotted against wavelength after white light was shone through the Fabry−Perot interferometer constructed by silvering the back-sides of the mica sheets. The experiments refer to the *same* sheet of cleaved mica, cut using surgical scissors to be particle-free: in one case to a portion that was never exposed to platinum wire, and in a second case to a portion that was exposed to glowing platinum wire to produce a surface density of ~2% nanoparticles. In both cases the mica sheet was subsequently cut in two, the dry halves were placed together as a sandwich, and the FECO fringes were imaged using a CCD (charge coupled detector). The main figure shows a single fringe, and the inset shows an expanded view of four fringes. Note that birefringence of mica causes each fringe to split into two component, β and γ.

with numerous experiments showing that both force−distance and shear properties vary systematically according to the molecular makeup of confined fluids (chain dimension, chain length, polarity).

Reflection shows that surface disorder is probably inevitable whenever surfaces are exposed to ambient atmosphere. Heterogeneity can be topographical and also chemical. In some sense, surely it is more representative than the hypothetically homogeneous surface chemical makeup and topographical structure that is sometimes assumed in this field of study. This study highlights its salient and interesting role.

Acknowledgment. We are indebted to Yingxi Zhu, Carlos Drummond, David Cahill, Les Allen, and Jianmin Zuo for discussions and advice, to Min Zhang and Jing Tao for assistance with TEM measurements, and to Mike Williams in the Center for Microanalysis of Materials for assistance with RBS measurements. This work was supported by the U.S. Department of Energy, Division of Materials Science, under Award No. DEFG02-91ER45439, through the Frederick Seitz Materials Research Laboratory at the University of Illinois at Urbana−Champaign.

LA034716U

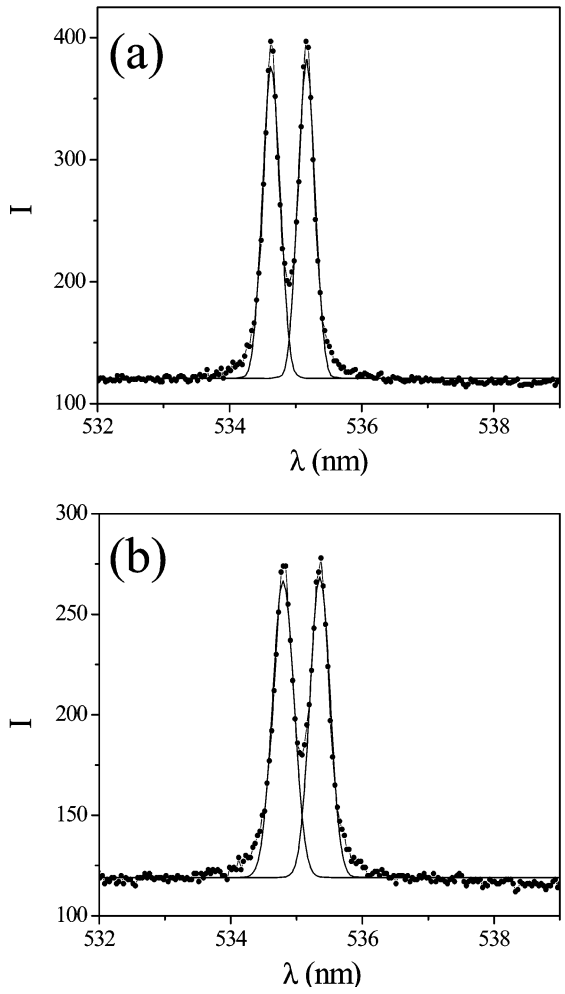

Figure 12. Gaussian fits of the interference fringes shown in the main part of Figure 11. For the β and γ fringes, respectively, the full widths at half-maximum (fwhm) were 0.26 and 0.25 nm (a, no particles present) and 0.32 and 0.30 nm (b, Pt nanoparticles present). Thus, although the particle spacing was less than the optical wavelength, particles manifested themselves in broadened fringes.